ACS APPLIED MATERIALS & INTERFACES

Research Article

www.acsami.org

Phyto-inspired Silica Nanowires: Characterization and Application in Lipase Immobilization

Ashit Rao,[†] Ashok Bankar,[†] Amul Shinde,[‡] Ameeta Ravi Kumar,[†] Suresh Gosavi,*[,‡] and Smita Zinjarde*[,†]

[†]Institute of Bioinformatics and Biotechnology and [‡]Department of Physics, University of Pune, Pune 411 007, India

ABSTRACT: Silica nanostructures were phyto-fabricated on different surfaces by using pomegranate (*Punica granatum*) leaf extracts. On zinc films, nanowires were obtained. On other surfaces such as silica, alumina, zinc oxide, and glass, spherical aggregates, cubic assemblies, microflakes, and acicular structures, respectively, were observed. The nanowires developed on Zn surfaces were characterized by scanning electron microscope-energy dispersive spectrometer (SEM-EDS), X-ray diffraction (XRD), photoluminescence, and Fourier transform infrared (FTIR) spectroscopic analysis. XRD profiles displayed peaks at 2.4, 4.9, and 12.1° indicating the presence of silica nanostructures. When excited at 340 nm, the reaction mixtures displayed a characteristic blue luminescence at 404 nm. FTIR spectra showed the existence of Si−OH and Si−O−Si bonds. The nanowires were functionalized with amine groups and used for the covalent immobilization of *Candida rugosa* lipase. The immobilized enzyme displayed better pH and temperature stability and retained 80% activity after 20 cycles. This paper highlights a novel route for the phyto-mediated growth of silica nanowires on Zn surfaces, their characterization and effective use as a matrix for enzyme immobilization.

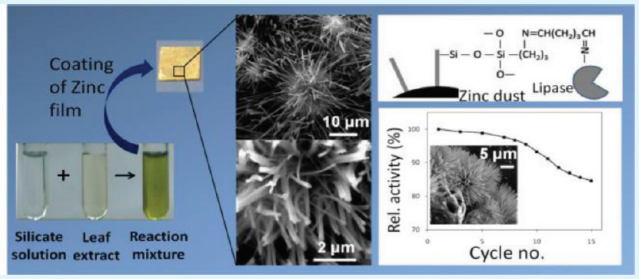

KEYWORDS: *Punica granatum, phyto-fabrication, silica nanowires, characterization, lipase immobilization*

INTRODUCTION

The synthesis of one-dimensional nanostructures such as nanowires and nanotubes has received considerable attention on account of the interesting optical and electronic properties that they display.[1] Among these, silica nanowires have been used in the construction of waveguides, biosensors, scanning near field optical microscopes, and other optical transmission devices.[2] Silica nanowires are conventionally synthesized by a variety of physical and chemical methods.[3,4] The aforementioned routes involve the use of specialized equipment, vacuum devices or metallic catalysts that often add to cost and energy-inputs.[5] Silica nanowires have also gained importance on account of their high mechanical strength.[6] Controlled organization of nanocrystals, high yields and clean processes are other significant features that need to be considered during the mass production of nanowires.[7] In view of this background, there is a need to explore alternative, green routes for the controlled synthesis of silica nanostructures.

In nature, diatoms, choanoflagellates, and sponges are known to process silicon. They synthesize biosilicates in hierarchical patterns via processes that occur at atmospheric pressure and ambient temperature.[8,9] Proteins, carbohydrates, lipids, metal ions and phenolic compounds have been proposed to mediate the formation of these patterned biosilicas.[8] Although isolated peptides and proteins derived from these biological systems have been employed for the *in vitro* synthesis of silica nanospheres,[10,11] to the best of our knowledge, there are no reports on the phyto-inspired synthesis of silica nanowires. In the present study, the leaf extracts of pomegranate (*Punica granatum*) mediated the synthesis of a variety of silica nanostructures on different surfaces. Silica nanowires were obtained by air-drying reaction mixtures on Zn wafers or dust under ambient conditions. The properties of these nanowires have been determined by employing a variety of analytical techniques. In addition, they have been used for the immobilization of a biotechnologically important enzyme "lipase". Lipases are known to hydrolyze a wide range of substrates with high enantio- and regio-selectivity.[12] In particular, the lipase from *Candida rugosa* has been extensively studied and is commercially available. The effect of the immobilization process on enzyme activity with respect to pH, thermal stability, kinetic parameters and recyclability has also been investigated.

MATERIALS AND METHODS

Materials. Sodium silicate ($Na_2SiO_3.9H_2O$) used for the synthesis of the nanostructures was obtained from Merck, Germany. 3-aminopropyltriethoxysilane (3-APTES), lipase (from *C. rugosa*), bovine serum albumin (BSA, molecular mass: 67 000 Da), and *p*-nitrophenyl palmitate (*p*-NPP) were purchased from Sigma. The chemicals were of analytical grade and were used as received. Millipore water (specific resistivity 18 M Ω cm) was used for the making all solutions. Zn dust on account of its higher surface to volume ratio (particle size <63 μm, Merck, Germany) was used as a template for

Received: November 5, 2011
Accepted: December 27, 2011
Published: December 27, 2011

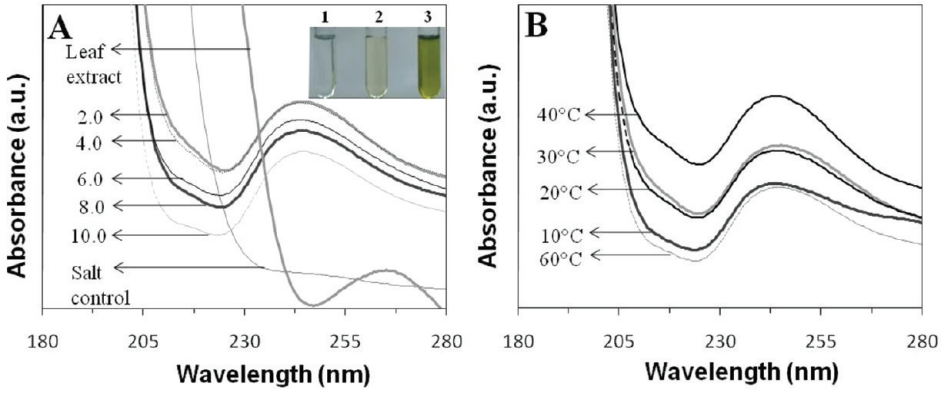

Figure 1. Visual observations and UV−visible spectra of reaction mixtures (containing leaf extract and 0.2 M sodium silicate in a 1:2 ratio) after 15 min. (A) At different pH values. Inset represents visual observations of (1) salt control without the leaf extract, (2) leaf extract without the salt, (3) a typical reaction mixture displaying a yellow color. (B) At different temperatures.

growing the silica nanowires during the enzyme immobilization experiments.

Synthesis of Silica Nanostructures. Leaves of *Punica granatum* were homogenized in a blender and extracted with water (1:10 w/v). The extract was centrifuged at 6000 *g* for 20 min. The supernatant was mixed with 0.2 M sodium silicate solution in a ratio of 1:2. The reaction mixture was incubated at 25 °C for 15 min. Different surfaces [silicon (1 1 1), alumina, ZnO, Zn (99.5%) wafers and glass slides] were coated by the drop cast method. A 50 μL drop of the reaction mixture was deposited on the surface and air-dried for 12 h. For enzyme immobilization studies, Zn dust (500 mg) was mixed with the reaction mixture (0.2 mL) in a Petri dish and incubated for 12 h under static conditions as described above.

Characterization of Nanostructures. UV−visible spectroscopy of the reaction mixtures at different pH and temperature conditions was performed on a Jasco V-530 spectrophotometer operated at a resolution of 1 nm. The pH of the reaction mixtures were adjusted to 2.0, 4.0, 6.0, 8.0, or 10.0 with 0.1 N HCl or NaOH solutions and nanostructure formation was monitored. The structural features of the coated surfaces were recorded by using an analytical SEM (JEOL JSM-6360A) equipped with EDS. XRD patterns were obtained on a D8 Advanced Bruker instrument with Cu Kα radiation (λ = 1.54 A°). Photoluminescence measurements were performed by using a Hitachi 2500 spectrofluorometer. The FTIR spectra were collected at a resolution of 4 cm^{-1} in the transmission mode (4000−400 cm^{-1}) by using a Shimadzu FTIR spectrophotometer (FTIR 8400). The contact angle analysis was done by the sessile water drop method using a Rame Hart 100 goniometer equipped with DROPimage Advanced software. The specific surface area was measured by using the Brunauer−Emmett−Teller (BET) technique with a Quantachrome NOVA 1200 equipment. The samples were heated to 200 °C for 1 h for removing adsorbed gases before starting the measurements. All experiments were performed in triplicates with two biological replicates and representative data or images are presented here.

Lipase Immobilization. The Zn microparticles coated with silica nanowires were used for immobilization of *C. rugosa* lipase. The nanowires were silanized with 3-aminopropyltriethoxysilane as described earlier.[13] The coated Zn particles (500 mg) were treated with 2.0 mL of 3-APTES in water (10%; pH 3.5). The samples were incubated for 8 h, rinsed gently with water and dried. The particles thus obtained were activated with 25% glutaraldehyde (25 mL/g of coated Zn dust). The mixture was stirred gently at 25 °C for 30 min and washed with deionized water. The activated silanized support was added to the enzyme solution (1 mg/mL; 40.0 mL) prepared in phosphate buffer (50 mM, pH 7.5) and incubated at 25 °C for 12 h with constant stirring. The loading capacities of the silica nanowires grown on Zn dust were also determined. The protein concentration in the immobilization reaction at time 0 and after 12 h was determined. The differences between these values were used to quantify the loading capacities. The protein contents were determined by the Bradford method and BSA was used as the standard protein.[14]

Determination of Enzyme Activity and Protein Content. The activity of the lipase preparation was determined according to a previous report.[15] The reaction mixtures consisted of 1.0 mL of *p*-NPP in ethanol (14.4 mM), phosphate buffer, (50 mM, pH 7.5) and appropriate contents of immobilized (10 mg) or free enzyme preparations. The mixtures were incubated for 15 min and the reactions were terminated by adding 0.5 mL of Na_2CO_3 (0.5 M) followed by centrifugation at 2,000 *g* for 10 min. Subsequently, the absorbance of the supernatant was measured at 410 nm by using a Thermo Multiskan ELISA reader. Reaction mixtures without the enzyme or substrate were treated as control experiments. The reaction rates were determined from the slopes of absorbance versus time plots. One unit of enzyme activity was defined as the quantity of the enzyme liberating 1.0 μM of *p*-nitrophenol (*p*-NP) per min at 40 °C and pH 7.5. For the immobilized enzyme, the specific activity was evaluated in terms of lipase units/g of the Zn support.

Properties of Free and Immobilized Enzymes. The effect of pH on the lipase activity was tested in phosphate buffer (pH 7.0, 7.5, 8.0, 8.5, and 9.0) after incubation at 35 °C for 15 min. The effect of temperature on lipase activity was determined at 35, 40, 50, and 60 °C at pH 7.5 and 8.0 for the free and immobilized forms, respectively. The thermal stability of the free and immobilized lipase was also determined by incubating the enzyme preparations at 50 or 60 °C. Samples were withdrawn at regular intervals and assayed for residual enzyme activity under optimum conditions (pH: 7.5 and 8.0; temperature: 40 and 50 °C for the free and immobilized forms, respectively). The reusability of the immobilized lipase was evaluated by centrifuging the reaction mixtures at 2000 *g* for 5 min. The immobilized lipase was washed with phosphate buffer, the samples were used to set up fresh assays and the residual activity was estimated. For these studies, the maximum lipase activity was considered as 100% and other values were depicted as relative units. In the graphs related to this data, mean values of triplicate experiments are plotted and error bars indicate standard deviation. The kinetic parameters (K_m and V_{max}) for the free and immobilized lipase preparations were calculated from the Lineweaver−Burk plots.[13] All experiments were run in triplicate and the arithmetic mean values were considered for data analysis.

RESULTS AND DISCUSSION

Visual Observations and UV−Visible Spectra. The inset in Figure 1 shows representative tubes of the salt control (tube 1) and the leaf extract control (tube 2). When the leaf extract was incubated with sodium silicate solution, a yellow color was observed (tube 3). Figures 1A and B show representative UV−visible spectra of the reaction mixtures after 15 min under different conditions of pH and temperature, respectively. The salt control did not show any peak and the leaf extract displayed

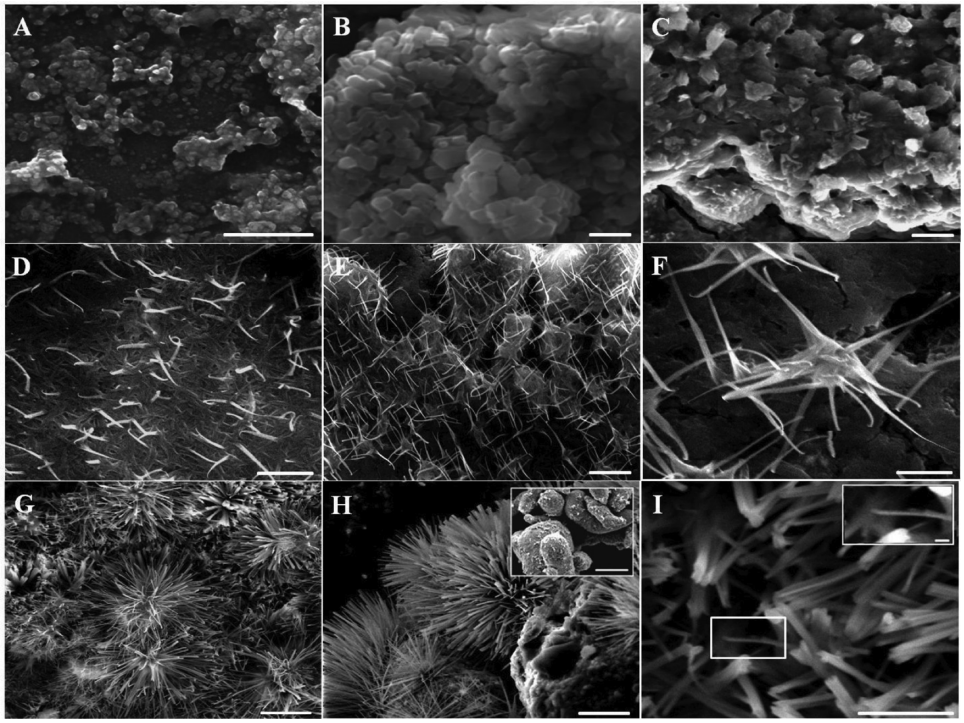

Figure 2. Representative SEM images of silica structures grown on (A) silica, (B) alumina, (C), zinc oxide, (D, E, F) glass, (G) zinc films, and (H, I) zinc dust. Bars represent (G) 20, (H) 5, (A, D, I) 2, and (B, C, E, F) 1 μm. Inset in image H represents unmodified Zn particles. Bar is equivalent to 10 μm. Inset in image I represents a magnified view of the marked area. Bar in the inset image is equivalent to 100 nm.

a peak at around 260 nm (Figure 1A). The reaction mixtures, however, displayed a peak at 244 nm. From Figure 1A, it is also evident that the intensity of the peaks decreased with an increase in pH. These results suggested the possible role of phenolic compounds in the synthetic process. The stability of such compounds often varies with pH. For example, gallic acid (present in *P. granatum*), caffeic and chlorogenic acids are known to be unstable at high pH values.[16] The studies on the effect of temperature (Figure 1B) showed that the maximum peak intensity was at 40 °C. All subsequent reactions were performed at pH 2.0 and 40 °C.

The absorption maxima wavelength (244 nm) observed in the current study is equivalent to a photon energy value of 5.1 eV. In an earlier investigation on the optical properties of silica, similar values of photon energy have been reported.[17] These results indicated that some components of the leaf extract mediated the reduction of silicate species (SiO_4^{4-}) to silica (SiO_2). A previous study has described the use of polyphenol-rich tea extracts for the reduction of metal ions to nanostructures.[18] *P. granatum* leaves are rich in gallic acid-based polyphenols such as ellagitannins and gallotannins, that display strong antioxidant (reductive) properties.[19−21] Such phenolic compounds are known to alternate between hydroxylated and quinone states thereby mediating redox reactions.[22] In the present investigation, the reduction of silicates to silica was possibly mediated by such phenolic compounds.

SEM-EDS, XRD, and Photoluminescence Studies. The silica nanostructures derived by air-drying the reaction mixtures on different substrates were analyzed by SEM (Figure 2). On silicon wafers, polydisperse particles were observed (Figure 2A). On alumina, cubic microaggregates were obtained (Figure 2B). Figure 2C shows micrometer-sized flakes on Zn oxide surfaces. Drying the reaction mixtures on glass surfaces led to the formation of acicular microstructures that were approximately 2 μm long (Figure 2D). These self-assembled to form star-shaped complexes (Figure 2E, F). Deposition of the reaction mixtures on Zn films and dust resulted in the formation of structures somewhat similar to those obtained on glass surfaces (Figure 2G, H). The structure of the Zn particles prior to silica coating is depicted in Figure 2H (inset). It is evident that the Zn surfaces were extensively modified after coating. The filaments assembled to form larger aggregates that displayed a better surface coverage compared to glass surfaces (Figure 2E, F). High-resolution images showed that the filaments were composed of thinner nanostructures (Figure 2I). The inset in Figure 2I shows that these filaments were less than 100 nm in thickness and hence could be considered as nanowires.[23] Chemically synthesized colloidal silica particles are reported to self-assemble on surfaces such as mica, glass, gold and silver into different structures. The patterns of self-assembly depended on the concentration of the particles, surface roughness, contact angle of the water droplet and the surface charge on the substrate.[24] In the current investigation also, pattern formation was dependent on the nature of the surface that was used for coating the samples. The significance of such bioinspired, self-assembly based routes for the facile synthesis of complex structures has been highlighted earlier.[25] The present study depicts a simple phyto-inspired method for synthesizing a variety of silica nanostructures under ambient conditions.

The EDS facility was used to validate the elemental composition of the nano structures grown on the Zn surface. A representative spot EDS profile is depicted in Figure 3. The profile showed signature peaks for silicon (black arrows) and oxygen. These results indicated that the nanowires were composed of silica.[26] To further characterize these nanowires, we took up XRD and PL studies.

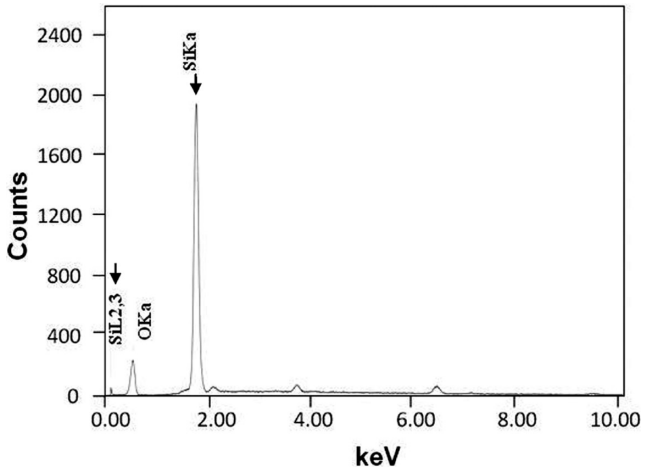

Figure 3. Representative EDS profile of silica nanowires on zinc wafers.

Figure 4A (1) shows a representative XRD pattern of the silica nanowires. A peak (arrow) was observed at 2.4°. In addition, broad peaks at 4.9 and 12.1° were also observed (arrow). The peak at 2.4° has also been reported earlier for the siliceous spicules produced by the demosponge *Thetya aurantium*. These spicules were proposed to be deposits of amorphous silica on repetitive protein template units and they displayed a "crystal-like" diffraction pattern.[27] The peaks (4.9 and 12.1°) have been indexed earlier to the (0 0 1) and (0 0 2) planes of polymer nanocomposites containing intercalated silicates.[28] In the present study also, residual silicates were possibly intercalated with some biopolymers and thus displayed this XRD pattern. To investigate the possible role of the biological molecules in the assembly of the silica nanowires, XRD patterns of heated (70 °C for 30 min) samples were recorded. This XRD profile displayed a variation in the intensity, sharpness and number of peaks [Figure 4A (2)]. A similar effect of high temperature on the XRD patterns of siliceous spicules from a marine sponge has been reported.[27] As discussed earlier, the ordered silica structures in this sponge were biosynthesized through periodic protein units that acted as templates. Hence the change in the XRD profiles was attributed to protein unfolding or the reorganization of the siliceous ordered patterns. In the present investigation also, certain biomolecules in the leaf extract possibly mediated growth of the silica nanowires. Photoluminescence spectra displayed a peak at 404 nm when excited at 340 nm (Figure 4B). Emission peaks in the range of 400−500 nm are characteristic of amorphous silica nanowires. These have been attributed to certain structural defects.[26]

Wettability Studies. To check the effect of the silica nanowire coating on Zn surfaces, water contact angle measurements were made. The nature of representative water droplets on Zn wafers prior to and after coating is shown in Figure 4C (1) and (2), respectively. For these samples, the contact angles were respectively calculated to be 82.4 ± 2.5 and 30.7 ± 1.3°. Other physical features such as the work of adhesion and spreading parameter also increased from 82.4 ± 3.2 to 135.4 ± 0.8 mN m^{-2} and −63.2 ± 3.2 to −10.44 ± 0.74 mN m^{-2}, respectively. Coating of Zn surfaces with silica nanowires thus increased their hydrophilic nature. This behavior is possibly due to the surface silanol groups in the

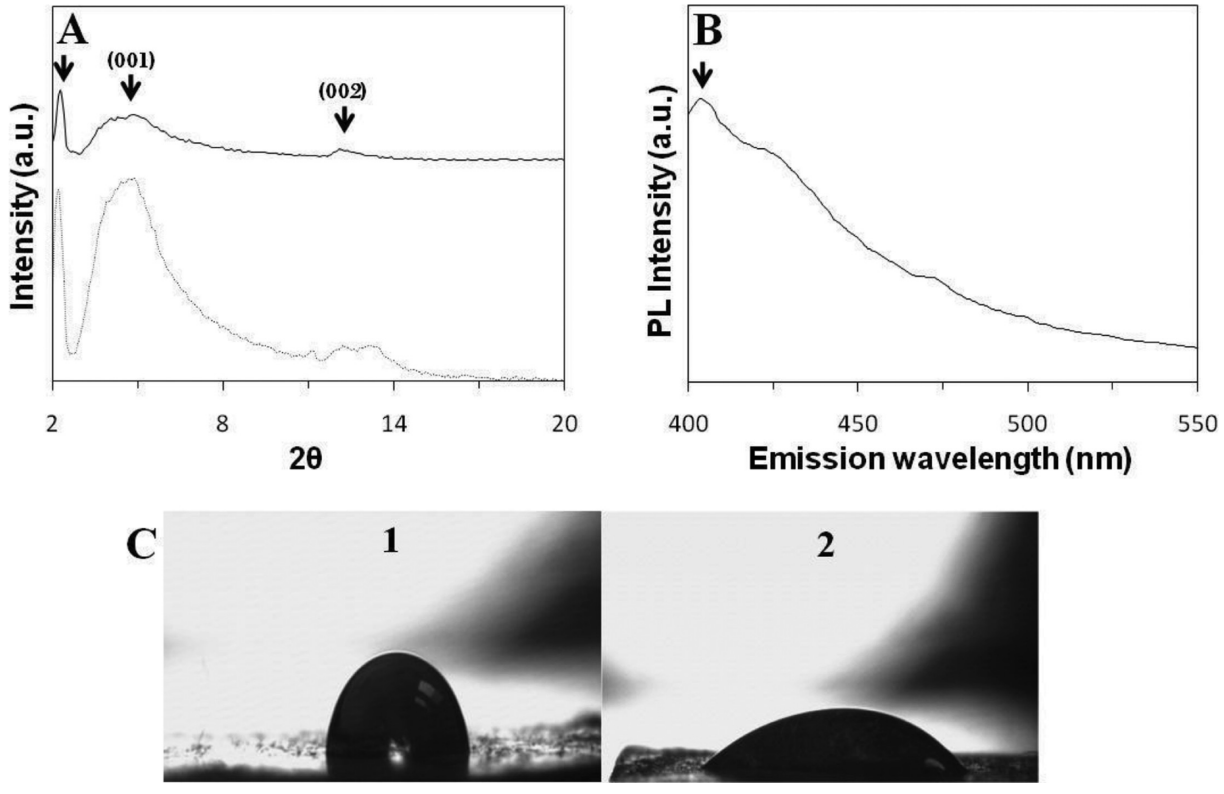

Figure 4. (A) Representative XRD profile of silica nanowires grown on zinc surface before (—) and after (····) heating at 70 °C for 30 min. (B) Representative photoluminescence spectra of reaction mixtures after excitation at 340 nm (C) Behavior of water droplets on (1) uncoated and (2) silica nanowire-coated Zn films.

dx.doi.org/10.1021/am201543e | *ACS Appl. Mater. Interfaces* 2012, 4, 871−877

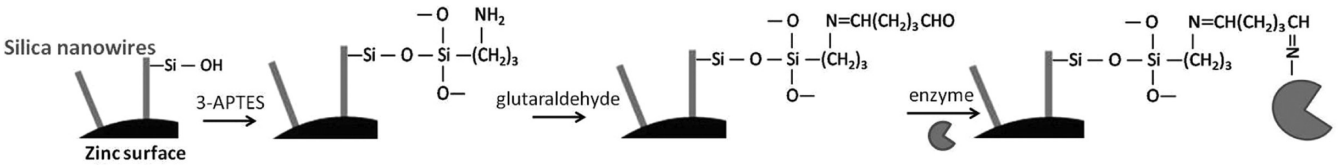

Figure 5. Schematic representation of reactions involved in the process of enzyme immobilization on the silica nanowires.

nanowires that had effectively covered the Zn films. The growth of the silica wires on Zn therefore resulted in (i) a considerable increase in the surface area (Figure 2H, I) and (ii) the presence of silanol groups which could be chemically modified for protein immobilization.

Silica Nanowire Matrix for Lipase Immobilization. Silica nanowire-coated Zn dust was evaluated for the immobilization of lipase, a biotechnologically relevant enzyme. On the basis of the BET experiments, the specific surface area of the uncoated Zn particles was estimated to be 5.78 m^2/g. This increased to 8.37 m^2/g after coating of the particles with the silica nanowires. As described in the experimental section and depicted in Figure 5, the covalent immobilization of lipase was achieved by the following steps (i) silylation of the hydroxyl group on the nanowires by 3-APTES (ii) transformation of the aminoalkyl group into Schiff's base by glutaraldehyde treatment (iii) covalent attachment of the amine group of the enzyme to the Schiff's base. The effectiveness of the silylation process was evaluated by FTIR analysis and the covalent immobilization was confirmed by the spectrophotometric lipase assay.

The representative FTIR spectra of the untreated and amino-functionalized silica nanowires are shown in Figure 6A. Prior to 3-APTES treatment (Figure 6A, 1), the spectra displayed a broad peak at 3400 cm^{-1}, characteristic of intra- and intermolecular hydrogen bonds of the silanol groups.[29] The peaks at 1083 and 2357 cm^{-1} were indicative of Si−O−Si stretching and Si−C triple bonds stretching, respectively.[30,31] Other peaks between 1300 and 1500 cm^{-1} could be attributed to vibrations of carbon atoms (possibly from the leaf extract) and suggested the existence of Si−OH and C−H deformations.[31] The FTIR spectrum after 3-APTES treatment is depicted in Figure 6A, 2. The two additional bands at 3417 and 1625 cm^{-1} could be attributed to the N−H stretching vibration and the bending mode of free NH_2 group, respectively. The peaks at 2930 and 2862 cm^{-1} were indicative of C−H stretching vibrations thereby confirming the anchorage of the propyl groups on the nanowire surface.[32] Some peaks in the 1300 and 1500 cm^{-1} range as well as the broad peak at 3400 cm^{-1} (representing silanol groups) were possibly masked due to the silanization process. The FTIR analysis thus confirmed an effective modification of the nanowires by 3-APTES. The amine functionalized nanowires were treated with glutaraldehyde (Figure 5), and these samples were incubated with different concentrations of lipase preparations as described in the experimental section. The enzyme immobilization procedure did not alter the morphology of the silica nanowires. Figure 6B is a representative SEM image of lipase immobilized silica-coated Zn dust sample and is comparable to the structures observed earlier (Figure 2G, H).

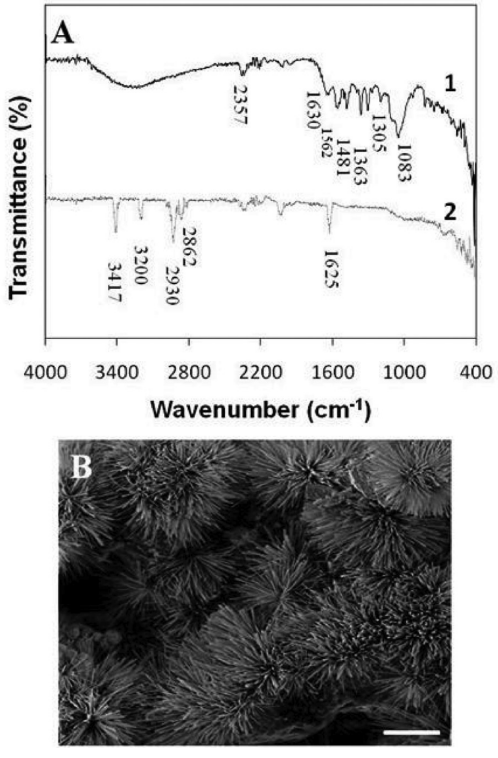

Figure 6. (A) Representative FTIR spectra of (1) unmodified (black) and (2) 3-APTES functionalized silica nanowires (gray). (B) Representative SEM image of silica nanowires with the immobilized lipase. Bar represents 10 μm.

Evaluation of Lipase Activity on the Silica Nanowire Coating. During immobilization experiments, the initial and final protein contents were estimated. On the basis of these values, the maximum lipase loading capacity was determined to be 63.5 ± 3.2 mg/g of the silica-coated Zn dust (Figure 7A). This is higher than earlier reported values for glutaraldehyde-mediated cross-linking. For example, the values of the optimal loading capacities for lipases derived from *Bacillus coagulans* and *C. rugosa* on Nylon-6 were 228 μg/g and 15 mg/g, respectively.[33,34] Other studies on the noncovalent immobilization of lipase have also indicated lower loading capacities in comparison to the present study. The values reported for the immobilization of *Mucor miehei* lipase by adsorption on MCM-41 matrix (100 A° pore size micelle template silica) as well as encapsulation in silica gel sol and sponge mesoporous silica are 9.9, 4.2, and 1.3 mg/g, respectively.[35] At the highest loading capacity (63.5 ± 3.2 mg/g), the enzyme activity of immobilized lipase in the present study was found to be 44 300 U/g. This value is higher than that reported for a silica clay material (palygorskite) wherein, the maximum activity was 3300 U/g.[13] A comparison of the loading capacities and enzyme activity values indicated that silica nanowire-coated Zn dust particles were efficient in lipase immobilization.

The performances of the free and immobilized lipases were evaluated. Studies on the effect of pH are shown in Figure 7B. The optimum pH for the free lipase was 7.5. For the immobilized form, this was extended between 7.5 and 8.0. The optimal reaction temperature for the free enzyme was 40

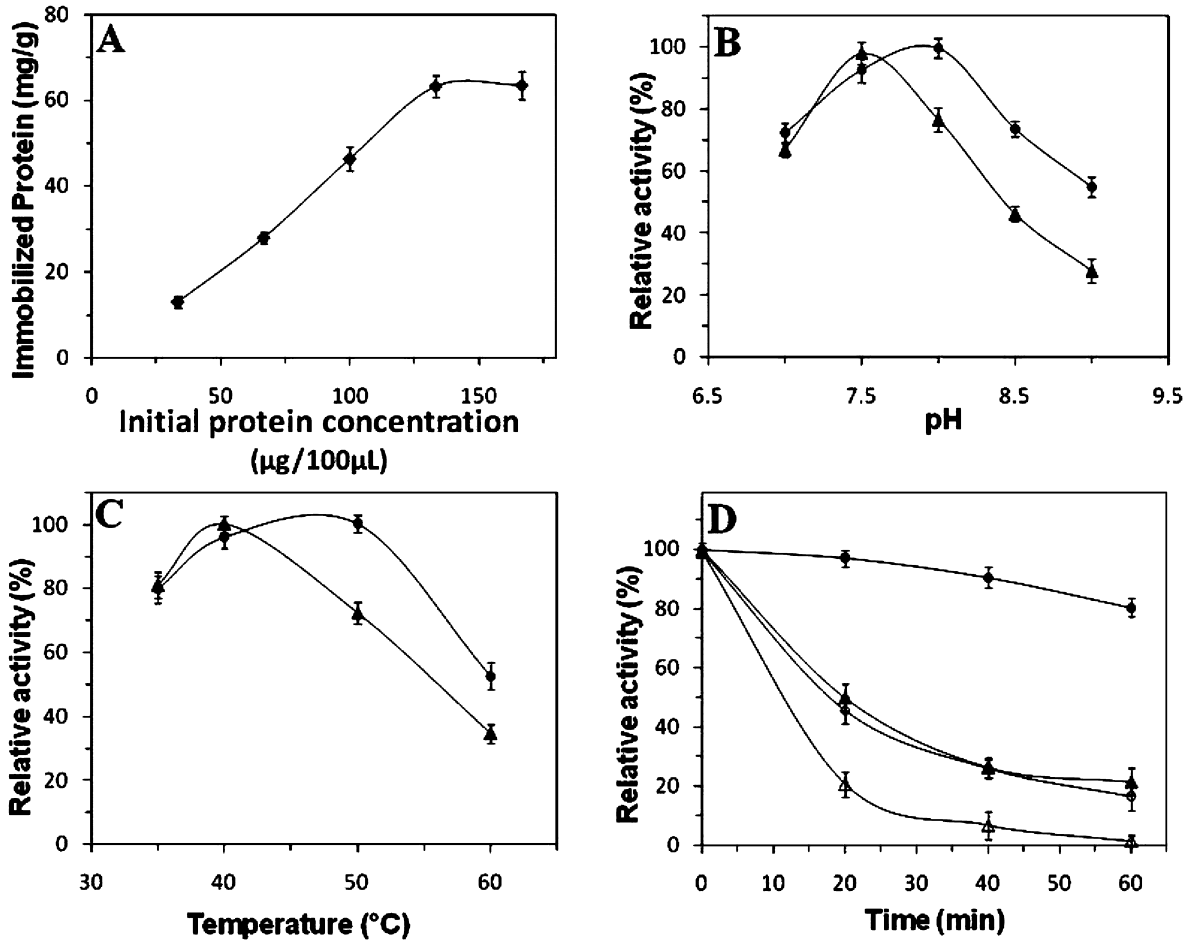

Figure 7. (A) Loading capacity of lipase immobilized on functionalized silica nanowires. Effect of (B) pH (C) temperature on activity of free (▲) and immobilized (●) enzyme. (D) Thermal stability of free (▲ 50 °C; Δ 60 °C) and immobilized (● 50 °C; ○ 60 °C) lipases.

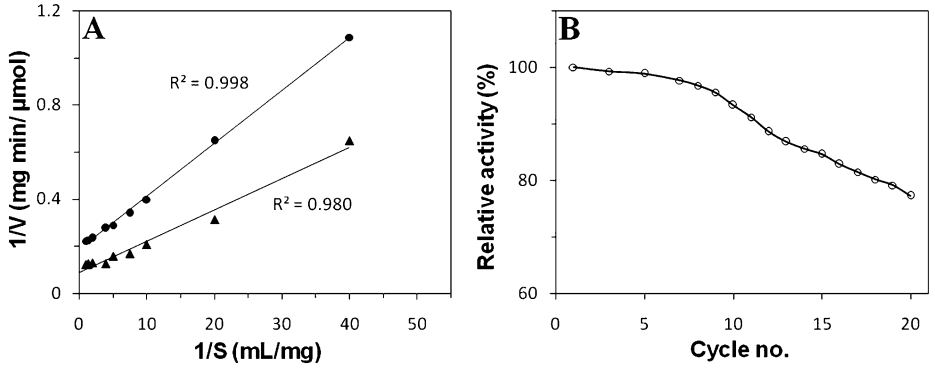

Figure 8. (A) Lineweaver–Burk plots of free (▲) and immobilized (●) lipase. (B) Residual activity after repeated use of the immobilized lipase.

°C (Figure 7C). The optimum temperature for the immobilized enzyme was in the range of 40–50 °C. These results indicated that the lipase immobilized on the silica nanowires were relatively less sensitive toward changes in pH and temperature compared to the free enzyme. Similar changes in pH and temperature optima for immobilized lipases have also been reported with other matrices such as chitosan and Nylon-6.[34,36]

The stability of the free and immobilized enzyme at 50 and 60 °C are depicted in Figure 7D. After 1 h at 60 °C, the residual activity of immobilized enzyme was found to be 21%. In comparison, the free enzyme displayed only 2% of residual activity. At 50 °C, the immobilized and free enzymes retained 80% and 16% activity, respectively, after 1 h of incubation. The immobilized lipase was thus relatively more stable than the free enzyme at the tested temperatures. Immobilized lipases from *C. rugosa* and *Candida lipolytica* are also reported to display increased thermal stability.[13,36] In addition, the lipase from *Bacillus coagulans* immobilized onto Nylon-6 fibers retained 88% of initial activity after 2 h of incubation at 55 °C.[33]

Kinetic constants for the immobilized and free enzymes with *p*-NPP as the substrate were calculated from Lineweaver–Burk

dx.doi.org/10.1021/am201543e | *ACS Appl. Mater. Interfaces* 2012, 4, 871–877

plots (Figure 8A). For immobilized lipase, the values of K_m and V_{max} were 310 μmol and 5.34 μmol/mg.mL and those for the free enzyme were 387 μmol and 1.23 μmol/mg.mL, respectively. The K_m and V_{max} values reported earlier for free lipase are 450 μmol and 46.4 μmol/(mg m)L, respectively.[15] The lower K_m value observed with the immobilized enzyme suggested the possibility of structural constraints that were introduced by the procedure of covalent immobilization.[36] In comparison to the free enzyme, the V_{max} value of the immobilized lipase was 4-fold higher. This could possibly be attributed to a favorable microenvironment that facilitated mass transfer of substrate or product to or from the active site of the enzyme.[15] The stability of the immobilized enzyme during continuous applications (20 cycles) was also evaluated. As shown in Figure 8B, the immobilized lipase retained about 80% of initial activity after 20 cycles. In comparison, the residual activity of *C. rugosa* lipase immobilized on chitosan-modified nanofibrous membrane was 55%.[15] In another study, *B. coagulans* lipase immobilized on glutaraldehyde-activated Nylon-6 retained 86 and 20.4% of initial activity after 8 and 13 cycles, respectively.[34] The increased recyclability in the present study may be due to a biocompatible microenvironment being provided by the chemically modified phytofabricated silica nanowires.

CONCLUSIONS

The present study describes the facile growth of a variety of silica structures on different surfaces using pomegranate leaf extract. By this simple, green method, silica nanowires could be synthesized on glass and Zn surfaces. The photoluminescence properties and surface functional groups were typical of silica wires. Since silica-based carriers are popular matrices for enzyme immobilization, the nanowire-coated Zn dust particles were used for covalent lipase immobilization. The maximum loading capacity was 63.5 ± 3.2 mg/g and the activity observed at this capacity was 44,300 U/g of the matrix. The pH and temperature optima were 8.0 and 50 °C, respectively. The immobilized lipase displayed enhanced temperature stability compared to the free enzyme. Comparison of the kinetic parameters indicated that the enzymatic reaction was facilitated by low mass transfer resistance. The phyto-fabricated silica nanowires thus synthesized were amenable to functionalization and could provide key insights for the controlled growth of one-dimensional nanoscale materials.

AUTHOR INFORMATION

Corresponding Author

*Tel.: + 91-20-25601385. Fax: + 91-20-25690087. E-mail: smita@unipune.ac.in; swg@physics.unipune.ac.in.

REFERENCES

(1) Shen, G.; Chen, P.; Ryu, K.; Zhou, C. *J. Mater. Chem.* **2009**, *19*, 828−839.
(2) Sood, D.; Sekhar, P.; Bhansali, S. *Appl. Phys. Lett.* **2006**, *88*, 143110.
(3) Sekhar, P. K.; Ramgir, N. S.; Joshi, R. K.; Bhansali, S. *Nanotechnology* **2008**, *19*, 245502.
(4) Park, S.; Heo, J.; Kim, H. *Nano Lett.* **2011**, *11*, 740−745.
(5) Luo, X.; Ma, W.; Zhou, Y.; Liu, D.; Yang, B.; Dai, Y. *Nanoscale Res. Lett.* **2010**, *5*, 252−256.
(6) Brambilla, G.; Payne, D. N. *Nano Lett.* **2009**, *9*, 831−835.
(7) Murphy, C. J.; Gole, A. M.; Hunyadi, S. E.; Orendorff, C. *J. Inorg. Chem.* **2006**, *45*, 7544−7554.
(8) Perry, C. *Rev. Miner. Geochem.* **2003**, *54*, 291−327.
(9) Coradin, T.; Lopez, P. J. *ChemBioChem* **2003**, *4*, 251−259.
(10) Kroger, N.; Deutzmann, R.; Sumper, M. *Science* **1999**, *286*, 1129−1132.
(11) Kroger, N.; Deutzmann, R.; Sumper, M. *J. Biol. Chem.* **2001**, *276*, 26066−26070.
(12) Schmid, R. D.; Verger, R. *Angew. Chem., Int. Ed.* **1998**, *37*, 1608−1633.
(13) Huang, J.; Liu, Y.; Wang, X. *J. Mol. Catal. B: Enzym* **2009**, *57*, 10−15.
(14) Bradford, M. *Anal. Biochem.* **1976**, *72*, 248−254.
(15) Ye, P.; Xu, Z.; Wu, J.; Innocent, C.; Seta, P. *Biomaterials* **2006**, *27*, 4169−4176.
(16) Friedman, M.; Jurgens, H. S. *J. Agric. Food Chem.* **2000**, *48*, 2101−2110.
(17) Nishikawa, H.; Shiroyama, T.; Nakamura, R.; Ohki, Y.; Nagasawa, K.; Hama, Y. *Phys. Rev. B: Condens. Matter Mater. Phys.* **1992**, *45*, 586−591.
(18) Nadagouda, M. N.; Castle, A. B.; Murdock, R. C.; Hussain, S. M.; Varma, R. S. *Green Chem.* **2009**, *12*, 114−122.
(19) Zhang, L.; Gao, Y.; Zhang, Y.; Liu, J.; Yu, J. *Sci. Hortic.* **2010**, *123*, 543−546.
(20) Nawwar, M. A. M.; Hussein, S. A. M.; Merfort, I. *Phytochemistry* **1994**, *37*, 1175−1177.
(21) Tanaka, T.; Nonaka, G. I.; Nishioka, I. *Phytochemistry* **1985**, *24*, 2075−2078.
(22) Duran, N.; Marcato, P. D.; Duran, M.; Yadav, A.; Gade, A.; Rai, M. *Appl. Microbiol. Biotechnol.* **2011**, *90*, 1609−1624.
(23) Xia, Y.; Yang, P. *Adv. Mater.* **2003**, *15*, 351−352.
(24) Ulmeanu, M.; Zamfirescu, M.; Medianu, R. *Colloids Surf., A* **2009**, *338*, 87−92.
(25) Whitesides, G.; Boncheva, M. *Proc. Natl. Acad. Sci. U.S.A.* **2002**, *99*, 4769−4774.
(26) Fang, X.; Ye, C.; Xie, T.; He, G.; Wang, Y.; Zhang, L. *Appl. Phys. A: Mater. Sci. Process* **2005**, *80*, 423−425.
(27) Croce, G.; Viterbo, D.; Milanesio, M.; Amenitsch, H. *Biophys. J.* **2007**, *92*, 288−292.
(28) Giannelis, E. *Adv. Mater.* **1996**, *8*, 29−35.
(29) Choi, S.; Lee, S.; Im, S.; Kim, S.; Joo, Y. *J. Mater. Sci. Lett.* **2003**, *22*, 891−893.
(30) Li, X.; He, Y.; Swihart, M. *Langmuir* **2004**, *20*, 4720−4727.
(31) Hamelmann, F.; Heinzmann, U.; Szekeres, A.; Kirov, N.; Nikolova, T. *J. Optoelectron. Adv. Mater.* **2005**, *7*, 389−392.
(32) Yamaura, M.; Camilo, R.; Sampaio, L.; Macedo, M.; Nakamura, M.; Toma, H. *J. Magn. Magn. Mater.* **2004**, *279*, 210−217.
(33) Zaidi, A.; Gainer, J. L.; Carta, G.; Mrani, A.; Kadiri, T.; Belarbi, Y.; Mir, A. *J. Biotechnol.* **2002**, *93*, 209−216.
(34) Pahujani, S.; Kanwar, S.; Chauhan, G.; Gupta, R. *Bioresour. Technol.* **2008**, *99*, 2566−2570.
(35) Galarneau, A.; Mureseanu, M.; Atger, S.; Renard, G.; Fajula, F. *New J. Chem.* **2006**, *30*, 562−571.
(36) Pereira, E.; Castro, H.; De Moraes, F.; Zanin, G. *Appl. Biochem. Biotechnol.* **2001**, *91*, 739−752.